Chemistry & Biology, Vol. 9, 215–224, February, 2002, ©2002 Elsevier Science Ltd. All rights reserved. PII S1074-5521(02)00097-2

Anchor-Based Design of Improved Cholera Toxin and *E. coli* Heat-Labile Enterotoxin Receptor Binding Antagonists that Display Multiple Binding Modes

Jason C. Pickens,[1,2,3,6] Ethan A. Merritt,[1,2,6] Misol Ahn,[1,2] Christophe L.M.J. Verlinde,[1,2] Wim G. J. Hol,[1,2,4] and Erkang Fan[1,2,5]
[1]Department of Biological Structure
[2]Biomolecular Structure Center
[3]Department of Chemistry
[4]Howard Hughes Medical Institute
University of Washington
Seattle, Washington 98195

Summary

The action of cholera toxin and *E. coli* heat-labile enterotoxin can be inhibited by blocking their binding to the cell-surface receptor GM1. We have used anchor-based design to create 15 receptor binding inhibitors that contain the previously characterized inhibitor MNPG as a substructure. In ELISA assays, all 15 compounds exhibited increased potency relative to MNPG. Binding affinities for two compounds, each containing a morpholine ring linked to MNPG via a hydrophobic tail, were characterized by pulsed ultrafiltration (PUF) and isothermal titration calorimetry (ITC). Crystal structures for these compounds bound to toxin B pentamer revealed a conserved binding mode for the MNPG moiety, with multiple binding modes adopted by the attached morpholine derivatives. The observed binding interactions can be exploited in the design of improved toxin binding inhibitors.

Introduction

Cholera toxin (CT) and heat-labile enterotoxin (LT) are two closely related protein toxins. Heat-labile enterotoxin is produced by enterotoxigenic *Escherichia coli* and causes traveler's diarrhea. Cholera toxin is produced by *Vibrio cholerae*, the causative agent of cholera, which frequently accompanies natural disasters and is endemic in parts of Asia. The two toxins share 80% sequence identity and have very similar structures and modes of action [1]. The proteins comprise one A subunit and five identical B subunits. The B subunits form a regular pentamer (LTB_5 or CTB_5) having five identical receptor binding sites, through which LT and CT interact with the receptor ganglioside GM1 (Galβ1-3GalNAcβ1-4(Neu5Acα2-3)Gal-β1-4Glc-ceramide) on the surface of human intestinal epithelial cells. LT and CT bind to the exposed GM1 oligosaccharide head group (GM1-OS, Figure 1) on the lumenal side of the intestinal epithelia (Figure 1). The toxin is then internalized via receptor-mediated endocytosis. Subsequently, the A subunit is transported to the cytosol, where it ADP-ribosylates the G protein $G_{s\alpha}$. Upon ADP-ribosylation, $G_{s\alpha}$ remains in its active form and continuously stimulates adenylate cyclase. The resulting increase in cAMP levels activates ion channels, causing a greatly enhanced efflux of ions and water into the intestinal lumen and leading to watery diarrhea [2].

One strategy for preventing the toxic activity of LT and CT is to block their entry into the host cells. Since GM1 binding by the toxins is a prerequisite for cell entry, one approach to developing small-molecule antagonists is to synthesize analogs of GM1-OS [3]. However, the synthesis of oligosaccharides, especially those containing the degree of branching and side-group modification found in GM1-OS, is synthetically very challenging and economically impractical [4]. Another approach is the de novo design of small-molecule antagonists. However, the shallow, solvent-exposed nature of the GM1 binding site makes such an approach difficult. Yet another alternative is to build off of a smaller carbohydrate element of the intact GM1-OS. One way to arrive at receptor binding antagonists is the use of a galactose "anchor," exploiting the fact that the terminal galactose of the natural receptor is important for binding [5, 6]. In a previous screening of 35 commercially available galactose derivatives, our group found *m*-nitrophenyl-α-D-galactopyranoside (MNPG, Figure 1) to be the most effective antagonist, with an IC_{50} of 0.6 mM in an LTB_5 ELISA assay [7]. The crystal structure of LTB_5:MNPG revealed that one of the oxygen atoms of the nitro group displaces canonical water #2 from the binding site to make a hydrogen bond with the backbone N-H of Gly33 (Figure 2) of a neighboring subunit in the pentamer. We have suggested that the increased entropy associated with the displacement of this water into bulk solvent accounts for a large part of the affinity gain [5].

For the design of improved antagonists, we decided to augment the favorable interactions of MNPG with CT and LT by building a new generation of small molecules based on the established MNPG scaffold. A collection of 15 compounds, containing a ring system connected by a short linker to the MNPG moiety, was synthesized and screened with an ELISA screening assay for the ability to block LTB_5 binding to an immobilized ganglioside receptor. Compared to MNPG, all 15 compounds exhibited enhanced potency. Additionally, two of the most potent antagonists were found to have much better aqueous solubility than the rest of the library and were further characterized by determining the binding constant (K_d) of the LTB_5 binding interaction via two different biophysical methods, isothermal titration calorimetry (ITC) and pulsed ultrafiltration (PUF). Compared to MNPG, both compounds display an increased affinity toward LT.

Crystal structures for both of these compounds bound to toxin were solved at high resolution, where a multiplicity of binding modes was observed. Together, the structure-activity relationships established by the two crystal structures and the improved solubility for the two compounds provide the basis for further structure-based optimization toward high-affinity antagonists targeting CT and LT.

[5]Correspondence: erkang@u.washington.edu
[6]These authors contributed equally to this paper.

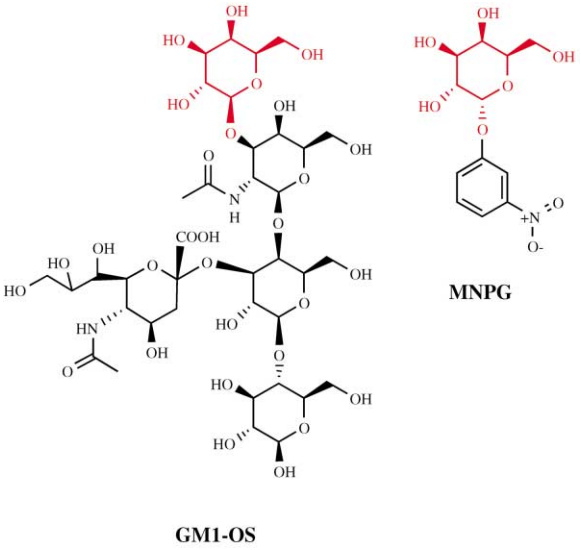

Figure 1. Chemical Features of GM1 and MNPG

Structures of the GM1 pentasaccharide (GM1-OS) and MNPG containing the galactose "anchor" (red).

Results and Discussion

Library Design

In order to explore regions of the GM1 binding site that are not involved in interactions with either GM1 or MNPG, we designed a small library of 15 compounds to incorporate a hydrophobic ring system linked via a short, flexible aliphatic linker through an amide linkage at the remaining *meta* position of the MNPG core (Figure 3). The crystal structures of MNPG bound to LT and CT [5, 8] showed that this position would be a good choice for the introduction of a new group because of its central location within the binding site. It was envisioned that, from this position, new groups could explore many different binding site regions, such as the pocket formed by Arg35, Tyr12, and Glu11, whereas *ortho* or *para* substitution would limit the possible number of locations explored (Figure 2). Additionally, we chose to investigate a range of linker lengths from 2–4 methylene units between the benzamide group and terminal ring system. We expected that this range of linker lengths would be sufficient to explore much of the remainder of the wide cleft that defines the GM1 binding site. The ring systems were chosen to represent several types, including aromatics, fused aromatics, and biphenyl, as well as saturated five and six-membered rings. In some cases, we duplicated the ring system but included a different number of methylene spacers in order to probe the effect of linker length.

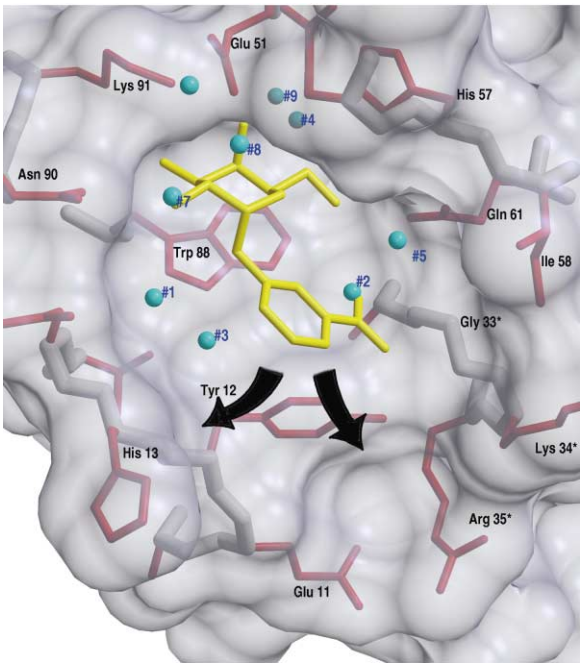

Figure 2. MNPG Bound to CTB_5

MNPG is in yellow. Arrows indicate unexplored regions of the GM1 binding site. Canonical water sites are shown as blue spheres. The canonical water at site # 2 is displaced by an oxygen atom of the nitro group. Ligand:toxin complexes in Figures 2, 5A, and 5B were rendered with *RASTER3D* [28].

Library Synthesis

Library synthesis and side chain selection is shown in Figure 3. After a batch $SnCl_4$-promoted glycosylation of 5-nitro-3-hydroxy-benzoic acid was performed on a multigram scale, the acetate-protected intermediate 3-carboxy-5-nitrophenyl-2,3,4,6-tetra-O-acetyl-galactopyranoside (CNPG) was split up and used without the removal of any unreacted pentaacetate starting material. Synthesis of the individual library members was conveniently performed in parallel via the method reported by Rayle and Fellmeth [9]; cyanuric chloride was employed as the carboxylic acid activating reagent, and various primary amines were used. We chose to use this particular activating agent because the cyanuric acid by-product can be easily and completely filtered away at the end of the reaction and anhydrous reaction conditions are not required, a particular concern to us since the CNPG intermediate is quite hygroscopic.

Because the $SnCl_4$-mediated glycosylation reaction is not stereoselective, the 15 compounds obtained after sugar deprotection and purification were each a slightly different mixture of α and β anomers (about 40% and 60%, respectively). The exact anomeric composition was determined by integrating the ^{1}H-NMR peaks corresponding to the anomeric protons for each product. It was assumed, based on our previous screening studies of commercially available galactose derivatives and crystal structure determinations, that the β anomer would contribute little to binding affinity in each of the library samples prepared [7]. For this reason, and also because separation of the anomers by silica gel chromatography and HPLC proved to be difficult, we screened the library with the anomeric mixture obtained after the HPLC purification. Milligram quantities of each of the compounds were obtained with purities greater than 90%, as estimated by inspection of ^{1}H-NMR spectra.

Library Screening

The library members were screened at a single concentration via the LTB_5 ELISA developed by Minke [7]. The

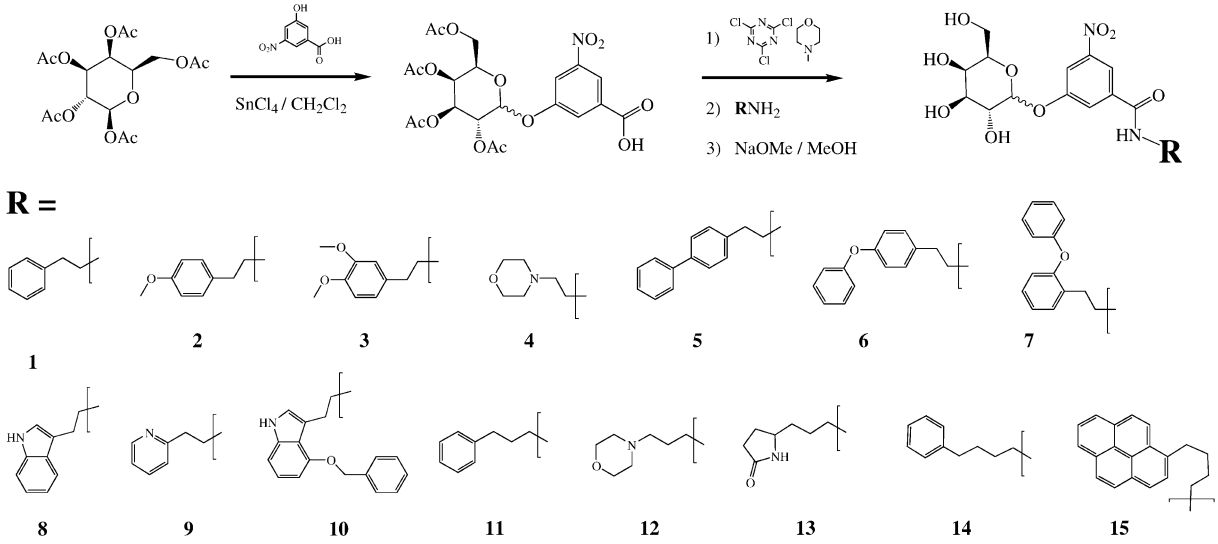

Figure 3. Solution-Phase Library Synthesis

Triazine-promoted amidation steps incorporating the various side chains and subsequent sugar deprotection steps were carried out in parallel. Linkers were two (**1–10**), three (**11–13**), or four (**14**, **15**) methylene units in length.

average concentration of the α anomer in each sample across all screened members was approximately 36 μM (100 μM total $\alpha + \beta$). Figure 4 shows that, at this concentration, all 15 of the compounds synthesized exhibit significant inhibition of LTB_5 binding. Based on the previously reported IC_{50} of 600 μM [7], the inhibition by α-MNPG at this concentration is less than 10%, whereas the library members display an average inhibition ranging from 20% to 55%. This narrow range of values seems to indicate that, within the variations tested, no strict preference for a particular linker length exists. Also, the fact that a high level of inhibition is displayed both by compounds containing saturated rings (**4** and **12**) and by aromatic systems (**5** and **6**) seems to indicate that new favorable binding interactions to the toxin B pentamer are introduced through the incorporation of either moiety into the MNPG anchor.

DMSO (10% by volume) was used in all samples to ensure uniform solubility. Without DMSO as a cosolvent, all of the compounds except for the tertiary amine-containing compounds **4** and **12** showed some degree of insolubility based on visual inspection of the ligand solutions prepared for an initial ELISA screening. Samples of the pyrene compound **15** showed cloudiness even in the presence of 10% DMSO, but they were still included in the final screening, where **15** showed the highest observed binding inhibition of all the compounds. It seems likely that, in this case, the extremely insoluble pyrene group combined with the longest linker length tested may induce toxin aggregation resulting in a false positive in the screening assay.

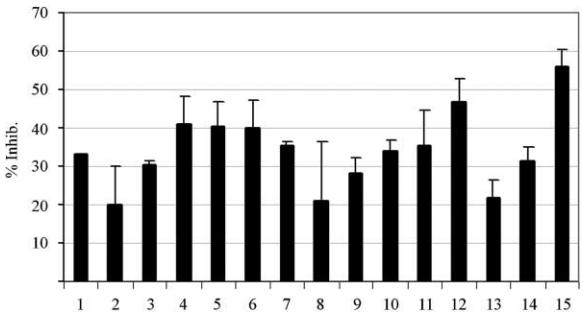

Figure 4. ELISA Screening Results

Inhibition of LTB_5 binding shown at an average α anomer concentration of 36 μM (100 μM total $\alpha + \beta$). Error bars indicate the standard deviation of two identical screening experiments. All 15 compounds show greater inhibition than the scaffold molecule MNPG, which in the same assay has an IC_{50} of 600 μM, corresponding to less than 10% inhibition at 36 μM.

Initial Crystallographic Analysis

Attempts to cocrystallize four of the most potent compounds, **4**, **5**, **11**, and **12**, with LTB_5 and CTB_5 have yielded crystals for all four. However, no data could be collected for compound **11** because the crystals obtained were too small to be useful. The structure of LTB_5 cocrystallized with the biphenyl compound **5** was solved to 1.8 Å resolution (our unpublished data). However, there is solid density only at a single site, where the biphenyl moiety extends directly out of the binding site to make interactions with a neighboring pentamer. This result is not of sufficient interest to be discussed further here. The structures of the morpholine-containing compounds **4** and **12** complexed to B pentamers are fortunately more interesting (Table 1), and we decided to focus our attention on these two compounds for a more detailed study because they are highly soluble in the aqueous buffers employed in our assay systems.

Observed Binding Modes of 4

Despite the increased affinity of compound **4** for the toxin receptor binding site relative to the galactose and MNPG substructures from which it was designed, no single conformation of the ethylmorpholine moiety pre-

Table 1. Crystallographic Statistics

Complex	LTB_5: 12	CTB_5: 4	
PDB accession code	1jqy	1jr0	
Space group	$P2_1$	C2	
	a = 65.0 Å	a = 102.1 Å	
	b = 166.0 Å	b = 66.1 Å	
	c = 74.4 Å	c = 78.6 Å	
	β = 92.3°	β = 105.7°	
Pentamers per asymmetric unit	3	1	
V_m (Å^3/Dalton)	2.1	2.2	
Data collection			
Unique data measured	84,223	110,275	
Completeness (highest shell)	97% (83%)	89% (40%)	
R_{merge} on intensities	0.050 (0.205)	0.048 (0.212)	
		isotropic	anisotropic
Data used in refinement			
Reflections (working set)	79,937	91,898	104,753
Reflections (R_{free} set)	4,235	4,927	5,513
Cutoffs	25–2.14 Å	22–1.4 Å	22–1.3 Å
Model			
R	0.2096	0.1868	0.1307
R_{free}	0.2879	0.2142	0.1834
Protein atom sites	12,360 B_{avg} = 38 Å^2	4,088	4,100 B_{avg} = 14 Å^2 $\langle A \rangle$ = 0.347
Ligand atom sites	462 B_{avg} = 63 Å^2	0	220 B_{avg} = 32 Å^2
Water molecules	1,096 B_{avg} = 39 Å^2	553	695 B_{avg} = 30 Å^2 $\langle A \rangle$ = 0.417
Sterochemistry			
Rms nonideality 1–2 distance	0.016 Å	0.010 Å	0.012 Å
Rms nonideality 1–3 distance	0.045 Å	0.025 Å	0.031 Å
Rms ΔB between bonded atoms	3.1 Å^2	2.1 Å^2	
Coord. ESU based on likelihood	0.21 Å	0.07 Å	
B ESU based on likelihood	8.0 Å^2	1.1 Å^2	

dominates in the crystal structure of the **4**:CTB_5 complex, which contained one pentamer per asymmetric unit (Figure 5A). Interpretation of the ($mF_o - F_c$) electron density at each of the five independent binding sites clearly indicated multiple conformational states of the bound ligand. The interpretability of the density was improved by refinement of an anisotropic model for the protein and well-ordered solvent molecules, with consequent overall improvement of model quality and residual difference density. Hand-fitting and real-space refinement into ($mF_o - F_c$) density at each binding site yielded one modeled conformation at two of the five independent binding sites and two conformations at each of the other three binding sites. All binding sites showed additional fragmentary density consistent with a mixture of several bound ligand conformations. All eight modeled conformations are shown superimposed onto the GM1 binding site in Figure 5A. Two major conformers are seen, differing by a 180° rotation about the bond between the benzene ring and the glycosidic oxygen of the galactose. In both conformations the water at the canonical binding site #2 has been displaced by an oxygen atom, either the carbonyl oxygen of the amide or one of the oxygen atoms of the nitro group. This displacement replicates the favorable binding mode first seen for MNPG. The ability to displace water #2 was a key design target for this series of compounds. The conformations seen for the terminal morpholine group variously place it in contact with different hydrophobic regions of the binding site, the largest contributors to which are the side chains of residues Glu11, Tyr12, Lys34, and Arg35. In particular, Tyr12 contributes to the interaction surface in most of the observed ligand conformations. Additionally, three ligand conformations are seen in which the morpholine ring interacts with Ile58, which is not involved in any interactions with the natural receptor GM1. This hydrophobic interaction likely contributes substantially to the overall affinity of compound **4**.

Observed Binding Modes of 12

The **12**:LTB_5 complex, with three pentamers per asymmetric unit, also exhibits a multiplicity of binding modes. Two major conformers are shown in Figure 5B. The observed difference electron density suggests that both conformers are present at each of the fifteen receptor binding sites, although only a single predominant conformation was modeled per site. As seen in the **4**:CTB_5 complex, the two conformations differ by a rotation about the sugar linkage to the central benzene ring. In this case, however, the difference in the torsion angle between the two conformers is roughly 120°. In conformer-1, predominant in five of the 15 crystallographically independent binding sites, the central benzene ring is positioned similarly to that in MNPG, with a consequent displacement of the water at site #2. In this conformer, the propyl chain linking the terminal morpholine ring extends along the side of the receptor binding pocket formed by Lys34. The position adopted by the amide carbonyl oxygen displacing the water at site #2 is stabilized by a hydrogen bond from the peptide nitro-

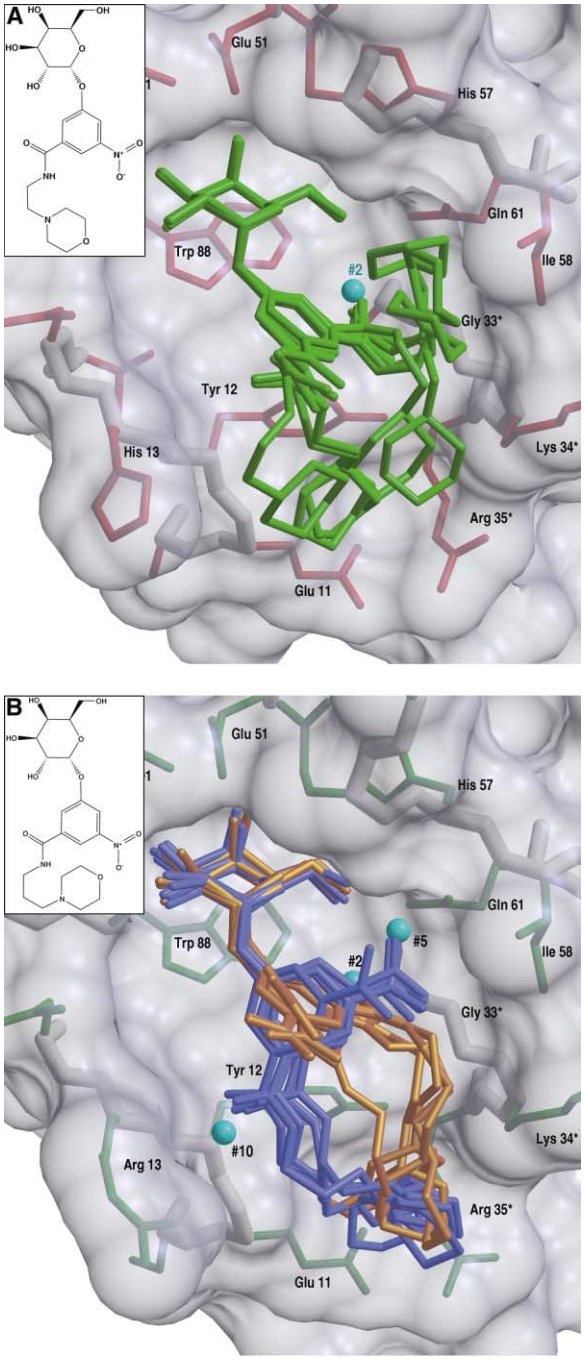

Figure 5. Structures of Ligands Bound with CT B Pentamer

(A) Superimposition of eight modeled conformations in the crystal structure of **4** bound to CTB_5. Two major conformers are observed to differ by a 180° rotation of the phenyl ring. In both conformations, the water at canonical site #2 (blue sphere) is displaced either by the amide carbonyl oxygen or the nitro group oxygen. Hydrophobic contact is made predominantly with Tyr12 in most conformations, as well as with Ile58 in three cases, but no well-defined consensus position for the morpholine ring is observed.

(B) Superimposition of the 12 modeled binding modes in the crystal structure of **12** bound to LTB_5. Two major conformers are seen. Conformer-1, shown in gold, displaces water #2 with the amide carbonyl oxygen while the nitro group points out of the binding site. In this conformer, the propyl linker makes hydrophobic contact with the side chains of Lys34 and Ile58. Conformer-2, shown in blue, hydrogen bonds with the peptide N-H of Arg13 and displaces water #10 on one side while the nitro group oxygen displaces water #5 on the opposite side. In both conformers, the morpholine ring resides in a pocket formed by the side chains of Arg35, Glu11, Lys34, and Tyr12.

gen of Gly33. A hydrogen bond network involving the water at site #5 further stabilizes it.

In conformer-2, modeled as predominating at seven of the 15 binding sites, the chain linking the terminal morpholine ring extends up the opposite side of the receptor binding site surface formed by residues Tyr12 and Arg13. Because the torsion angle distinguishing the two conformers is 120° rather than 180°, neither the nitro group nor the amide carbonyl oxygen displaces the water at site #2. Instead, the nitro group on one side displaces the water at site #5, and the amide carbonyl oxygen on the other side displaces the water at site #10. The nitro group position is stabilized by hydrogen bonding to the water at site #2; the amide oxygen position is stabilized by hydrogen bonding to the peptide nitrogen of residue Arg13 and to the water at site #3.

Both conformations place the terminal morpholine ring of **12** in approximately the same portion of the receptor binding site, where it interacts primarily via hydrophobic interactions with the side chains of Tyr12, Lys34, and Arg35. The difference electron density is not clear enough to allow us to model the precise conformation or orientation of the morpholine ring with confidence, and the flexibility of the chain linking it to the MNPG anchor is sufficient to allow a range of possible positions against the binding surface of the protein. In the crystal structure, local lattice interactions may introduce slight differences in the energetically favored conformations at each binding site, reflected both by the presence of different predominating conformers at different binding sites and by the variation within the refined models for the multiple examples of each ligand conformer. At two of the 15 binding sites, the presence of a nearby hydrophobic surface from a noncrystallographic symmetry (NCS)-related toxin pentamer sufficiently perturbs the local environment so that the terminal morpholine ring is observed not to lie along the receptor binding surface but rather against the NCS-related surface. An important point to note is that, although a mixture of α and β anomers was used in the crystallization experiments, only the α anomer is observed in the crystal structure for both compounds. This is consistent with the observation that the α anomer of MNPG interacts more favorably than the β anomer with the toxin B pentamer when they are assayed separately [7].

Binding Constants for Compounds 4 and 12

Intrigued by the crystal structures obtained for **4** and **12**, we decided to investigate more thoroughly the interaction of these two compounds with LTB_5 by using anomerically pure samples of each. Samples of **4** and **12** of purely α anomeric composition were obtained by resynthesizing the compounds and then treating each of the α/β mixtures obtained with immobilized β-galac-

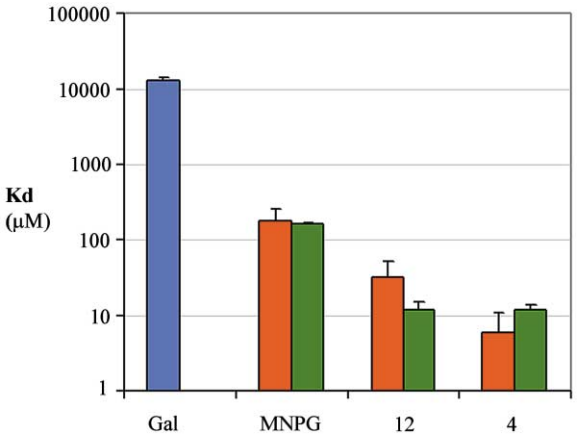

Figure 6. Comparison of Dissociation Constants Measured by Different Methods

Dissociation constants determined by ITC (green) and PUF (red). The previously reported K_d for β-galactose (blue) was determined by fluorescence spectroscopy [7]. Error bars indicate the standard deviation of at least two independent determinations. LTB_5 was the protein component used in all experiments.

tosidase followed by HPLC repurification to remove the by-products of the β anomer hydrolysis reaction.

We then used pulsed ultrafiltration (PUF) [10] and isothermal titration calorimetry (ITC) to determine the dissociation constants. We chose to use two different biophysical methods to help ensure accuracy in our measurements as well as for crossvalidation purposes.

The average K_d values from several experiments of each type along with values for MNPG and β-galactose for comparison are shown for **4** and **12** in Figure 6. A K_d value of 12 μM was found for both compounds via ITC. This corresponds to a 14-fold improvement over MNPG, which has a K_d value of 175 μM. The PUF experiments, with average values of 6 and 32 μM for compounds **4** and **12**, respectively, gave values that, in general, are in the same range as those obtained with ITC. The best agreement was obtained for the MNPG assays, where the difference in the K_d value obtained with the two techniques differed by less than 10%. Since PUF is a relatively new technique (compared to ITC) for measuring protein-ligand affinity, and since there are few references existing in the current literature, it may be that some of the limitations of the method and/or techniques for minimizing experimental error have not been well established. In fact, with the exception of the initial method development studies by Chen and coworkers [10, 11], this study is the first to our knowledge to report K_d values obtained by PUF. All other work cited in the literature is related to the use of PUF as a qualitative ligand-screening method [12–14]. The results we obtained indicate that PUF is a good method for obtaining K_d values associated with protein/ligand interactions, especially considering the small amount of both protein and ligand required, as well as the simplicity of data collection and analysis compared to ITC.

The observation that both compounds seem to have essentially the same affinity for LTB_5 can now be discussed in light of the two crystal structures, which reveal binding modes that are clearly distinct from each other. The bound conformations of **4** and conformer-1 of **12** retain the entropically favorable displacement of the water molecule at water site #2, as intended. Somewhat unexpectedly, conformer-2 of **12** instead displaces two other water molecules, those at water sites #5 and #10 (Figure 5B). At all three water sites, the hydrogen-bonding network involving the displaced water molecule is maintained by the corresponding ligand oxygen that displaces it. Perhaps the displacement of these two waters is roughly equivalent, energetically speaking, to the displacement of the water molecule at water site #2, but such a hypothesis would be difficult to establish experimentally.

The contribution of the linkers may also play a role in ligand affinity. The shorter ethyl group of **4** is not quite long enough to allow the terminal morpholine ring to reach a consensus position against the binding surface as in the case of **12**. It can, however, adopt a range of conformations placing it against an extended hydrophobic surface of the binding site, of which Tyr12 is only one part. By contrast, the slightly longer propyl linker of **12** allows favorable interaction of the terminal morpholine group and the linker itself with Tyr12 and Lys34 in both of the two observed predominant conformers. In fact, it might seem somewhat surprising that the two compounds have nearly equal affinity for the toxin pentamer since the propyl linker of **12** has an additional rotatable bond. One would expect that the greater degree of flexibility would lead to a greater loss of entropy upon ligand binding and hence lower the affinity. Counteracting this, however, is the fact that compound **12** buries a larger region of relatively hydrophobic surface on the binding site. The observed area of buried solvent-accessible surface (SAS) in the crystal structures (averaged over all modeled conformers) is 190 $Å^2$ for compound **4** and 230 $Å^2$ for **12**. The increase in binding affinity for **12** due to the 20% greater buried hydrophobic surface may act to compensate for the greater loss of entropy upon ligand binding.

In summary, the crystal structures of the **4**:CTB_5 and **12**:LTB_5 complexes confirm that anchor-based design of ligands with increased affinity for the toxin receptor binding site is feasible. Key favorable binding interactions observed for the anchor compound MNPG are retained by both of these ligands while the hydrophobic group linked to the MNPG anchor introduces additional favorable interactions with the targeted hydrophobic regions of the receptor binding site. Furthermore, the demonstration that the anchoring MNPG group can be extended through the addition of relatively flexible moieties without the loss of binding affinity is very encouraging. Such extension underlies the approach to generating extremely high-affinity multivalent antagonists to receptor binding by CT/LT [15, 16] and related toxins with even greater numbers of binding sites [17].

Significance

The diarrheal diseases caused by cholera toxin and *E. coli* heat-labile enterotoxin continue to contribute in large part to the total number of infectious disease-

related deaths each year. Currently, no prophylaxis is available for either toxin, and the efficacy of the vaccine against *V. cholerae* is short lived. In an effort to develop small-molecule antagonists of the receptor binding activity of CT and LT, a small library of compounds was designed and synthesized based on a previously characterized lead by using an anchor-based approach. An ELISA assay was used to screen the compounds for the ability to block toxin binding. All of the library members showed some degree of improvement in affinity over the lead, and two in particular were found to have good aqueous solubility, making them amenable to further characterization. The measured binding constants for these two compounds show both to have an approximately 14-fold affinity gain over the lead. The crystal structures of both compounds in complex with the target protein B pentamer were solved and showed multiple binding modes within the receptor binding site. In some instances, the inhibitor interacts with a protein residue that is not involved in interactions with the natural receptor. These results indicate that an anchor-based exploration of a protein active site is a viable approach to improving ligand affinity. Additionally, combined with the two compounds' improved affinity and solubility, the multiple binding modes displayed in their crystal structures may provide several new starting templates for the design of future mono- or multivalent inhibitors of CT and LT receptor binding.

Experimental Procedures

Synthetic Chemistry

General

Unless otherwise noted, all chemical reagents were purchased from Aldrich Chemical Co. and were used without further purification. All solvents used were obtained from Fisher Scientific (HPLC grade) and were used without further purification. ^{1}H-NMR spectra were obtained at 300 MHz in methanol-d_4 on a Bruker AC-300 instrument without sample spinning unless otherwise noted. Electrospray mass spectra were obtained with a Bruker Esquire electrospray mass spectrometer operating in negative ion mode. Reported m/z values refer to the molecular anion ($[M-H]^-$) unless otherwise noted. Preparatory HPLC purification of library compounds and pulsed ultrafiltration experiments were performed on a Hewlet-Packard 1100 Series HPLC system. Purification employed a Vydac brand 22 $\times$ 250 mm, 10 –15 μm pore size, C18 column equipped with a guard. Gradient elution was achieved with a 0.1% aqueous trifluoroacetic acid (TFA)/acetonitrile solvent system.

Library Synthesis

After our general procedure previously reported for the synthesis of phenyl-galactosides [8, 18], 3-hydroxy-5-nitrobenzoic acid (Impamex, Hartsdale, NY), (3 g, 16 mmol) and β-D-galactosepentaacetate were dissolved in 150 ml dry dichloromethane under nitrogen atmosphere. Anhydrous $SnCl_4$ (2 ml, 20 mmol) was added via syringe. The solution was refluxed under nitrogen for 72 hr and then cooled to room temperature. The reaction was quenched by the addition of 200 ml water while being vigorously stirred. The organic layer was washed five times with 200 ml of water to remove any residual phenol. The organic layer was then filtered through a cotton plug or celite 454 to remove insoluble tin salts and washed once with brine, dried over $MgSO_4$, and concentrated to yield 3.3 g (40% crude yield) of a pale-yellow solid, 3-carboxy-5-nitrophenyl-2,3,4,6-tetra-O-acetyl-galactopyranoside. This material was then divided into 200 mg portions and was used without further purification for the synthesis of individual library members. A typical example follows:

(3-nitro-5-(3-phenylethylaminocarbonyl)phenyl)-galactopyranoside (**1**): crude CNPG (200 mg, 0.38 mmol) was dissolved in 15 ml ethyl acetate. Cyanuric chloride (24 mg, 0.33 equivalents) was then added while the mixture was stirred vigorously. N-methylmorpholine (122 μl, 1 equivalent) was then added. A dense white precipitate formed. The mixture was allowed to stir for 1 hr, and then 2-phenylethylamine (46 μl, 0.388 mmol) was added. The mixture was allowed to stir for an additional 6 hr. The mixture was then filtered through a syringe filter (Titan brand, 2 μm nylon) to remove the precipitated cyanuric acid. The organic layer was washed twice with aqueous 5% citric acid, then twice with saturated aqueous $NaHCO_3$ and finally once with brine. The solvent was then removed by evaporation under vacuum. The acetate sugar-protecting groups were removed by redissolving the sample in 10 ml of a solution of 100 mM sodium methoxide in methanol. The solution was neutralized, and Na^+ was removed by passage through a 5 ml column containing cation exchange resin (Dowex 50 W, 8% crosslinking, strongly acidic cation) and then subjected to preparative HPLC purification. The major eluting peak was collected and concentrated to give 13 mg of **1** (7% overall yield, α:β = 33%:67%). ESI-MS m/z 447.3. ^{1}H-NMR: δ 8.83 (s, 1H, NH), 8.34 (s, 1H, aromatic, β anomer), 8.21 (s, 0.4H, aromatic, α anomer), 8.15 (s, 0.6H, aromatic, β anomer), 7.98 (s, 0.4H, aromatic, α anomer), 7.93 (s, 0.6H, aromatic, β anomer), 7.38–7.7.24 (m, 5H, phenyl), 5.75 (d, 0.4H, anomeric, β proton), 5.08 (d, 0.6H, anomeric, α proton), 4.07–3.81 (m, 6H, sugar), 3.71 (t, 2H, CH_2), and 3.00 (t, 2H, CH_2).

(3-nitro-5-(2-(4-methoxy-phenyl)-ethylaminocarbonyl)phenyl)-galactopyranoside (**2**): compound **2** was synthesized and purified in a manner analogous to the synthesis of **1**, with 2-(4-methoxyphenyl)ethylamine (Avocado research chemicals, 0.388 mmol) as the amine component. Yield: 12 mg (6% overall, α:β = 32%:68%). ESI-MS m/z 477.0. For ^{1}H-NMR, all peaks corresponding to the core structure were observed and were consistent with those reported for compound **1** with the following additional peaks observed for the side chain: δ 7.23 (d, 2H, aromatic), 6.92 (d, 2H, aromatic), 3.85 (s, 3H, O-CH_3), 3.64 (t, 2H, CH_2), and 2.93 (t, 2H, CH_2).

(3-nitro-5-(2-(3,4-dimethoxy-phenyl)-ethylaminocarbonyl)phenyl)-galactopyranoside (**3**): compound **3** was synthesized and purified in a manner analogous tothe synthesis of **1**, with 2-(3,4-dimethoxyphenyl)ethylamine (0.388 mmol) as the amine component. Yield: 17 mg (9% overall, α:β = 30%:70%). ESI-MS m/z 507.0. For ^{1}H-NMR, all peaks corresponding to the core structure were observed and were consistent with those reported for compound **1** with the following additional peaks observed for the side chain: δ 6.96-6.85 (m, 3H, aromatic), 3.87 (d, 6H, O-CH_3 $\times$ 2), 3.67 (t, 2H, CH_2), and 2.94 (t, 2H,CH_2).

(3-nitro-5-(2-morpholin-4-yl-ethylaminocarbonyl)phenyl)-galactopyranoside (**4**): compound **4** was synthesized and purified in a manner analogous to the synthesis of **1**, with N-(2-aminoethyl)morpholine (0.388 mmol) as the amine component. Yield: 16 mg (9% overall, α:β = 38%:62%). ESI-MS m/z 456.2, 569.9 (TFA adduct). For ^{1}H-NMR, all peaks corresponding to the core structure were observed and were consistent with those reported for compound **1** with the following additional peaks observed for the side chain: δ 3.86 (br t, 6H) and 3.49 (br t, 6H, CH_2).

(3-nitro-5-(2-biphenyl-4-yl-ethylaminocarbonyl)phenyl)-galactopyranoside (**5**): compound **5** was synthesized and purified in a manner analogous to the synthesis of **1**, with 2-(4-biphenyl)ethylamine (Transworld Chemicals, 0.388 mmol) as the amine component. Yield: 20 mg (12% overall, α:β = 42%:58%). ESI-MS m/z 523.0. For ^{1}H-NMR (acetone-d_6), all peaks corresponding to the core structure were observed and were consistent with those reported for compound **1** with the following additional peaks observed for the side chain: δ 7.71–7.65 (m, 4H, aromatic), 7.53–7.39 (m, 5H, aromatic), 3.78 (br t, 2H, CH_2), and 3.06 (t, 2H, CH_2).

(3-nitro-5-(2-(4-phenoxy-phenyl)-ethylaminocarbonyl)phenyl)-galactopyranoside (**6**): compound **6** was synthesized and purified in a manner analogous to the synthesis of **1**, with 4-phenoxy-phenethylamine (Transworld Chemicals, 0.388 mmol) as the amine component. Yield: 17 mg (10% overall, α:β = 41%:59%). ESI-MS m/z 539.0. For ^{1}H-NMR (acetone-d_6), all peaks corresponding to the core structure were observed and were consistent with those reported for compound **1** with the following additional peaks observed for the side chain: δ 7.42–7.35 (m, 4H, aromatic), 7.16 (t, 1H, aromatic), 6.98–7.10 (m, 4H, aromatic), 3.72 (br t, 2H, CH_2), and 3.01 (t, 2H, CH_2).

(3-nitro-5-(2-(2-phenoxy-phenyl)-ethylaminocarbonyl)phenyl)-

galactopyranoside (**7**): compound **7** was synthesized and purified in a manner analogous to the synthesis of **1**, with 2-phenoxyphenethylamine (Transworld Chemicals, 0.388 mmol) as the amine component. Yield: 9 mg (5% overall, α:β = 43%:57%). ESI-MS m/z 538.9. For ^{1}H-NMR (acetone-d_6), all peaks corresponding to the core structure were observed and were consistent with those reported for compound **1** with the following additional peaks observed for the side chain: δ 7.46–7.37 (m, 3H, aromatic), 7.30 (t, 1H, aromatic), 7.27–7.12 (m, 2H, aromatic), 7.0 (d, 2H, aromatic), 6.95 (d, 1H, aromatic), and 3.79–3.74 (m, 4H, CH_2).

(3-nitro-5-(2-(3aH-indol-3-yl)-ethylaminocarbonyl)phenyl)-galactopyranoside (**8**): compound **8** was synthesized and purified in a manner analogous to the synthesis of **1**, with tryptamine (0.388 mmol) as the amine component. Yield: 24 mg (13% overall, α:β = 40%:60%). ESI-MS m/z 486.2, 600.0 (TFA adduct). For ^{1}H-NMR, all peaks corresponding to the core structure were observed and were consistent with those reported for compound **1** with the following additional peaks observed for the side chain: δ 7.65 (d, 1H, aromatic), 7.4 (d, 1H, aromatic), 7.18–7.12 (m, 2H, aromatic), 7.05 (t, 1H, aromatic), 3.75 (br t, 2H, CH_2), and 3.15 (t, 2H, CH_2).

(3-nitro-5-(2-pyridin-2-yl-ethylaminocarbonyl)phenyl)-galactopyranoside (**9**): compound **9** was synthesized and purified in a manner analogous to the synthesis of **1**, with 2-(2-aminoethyl)pyridine (0.388 mmol) as the amine component. Yield: 30 mg (18% overall, α:β = 34%:66%).ESI-MS m/z 638.0 (TFA adduct). For ^{1}H-NMR, all peaks corresponding to the core structure were observed and were consistent with those reported for compound **1** with the following additional peaks observed for the side chain: δ 8.82 (s, 1H, aromatic), 8.58 (s, 1H, aromatic), 8.07 (d t, 1H, aromatic), 8.00 (s, 1H, aromatic), 3.93 (t, 2H, CH_2), and 3.44 (t, 2H, CH_2).

(3-nitro-5-(2-(4-benzyloxy-3aH-indol-3-yl)-ethylaminocarbonyl) phenyl)-galactopyranoside (**10**): compound **10** was synthesized and purified in a manner analogous to the synthesis of **1**, with 7-benzyloxytryptamine (0.388 mmol) as the amine component. Yield: 12 mg (6% overall, α:β = 40%:60%). ESI-MS m/z 591.9. For ^{1}H-NMR, all peaks corresponding to the core structure were observed and were consistent with those reported for compound **1** with the following additional peaks observed for the side chain: δ 7.59 (d, 2H, aromatic), 7.47–7.35 (m, 3H, aromatic), 7.27 (d, 1H, aromatic), 7.14 (s, 1H, aromatic), 6.96 (t, 1H, aromatic), 6.76 (d, 1H, aromatic), 5.29 (s, 2H, benzylic CH_2), 3.78 (br t, CH_2), and 3.13 (t, 2H, CH_2).

(3-nitro-5-(3-phenyl-propylaminocarbonyl)phenyl)-galactopyranoside (**11**): compound **11** was synthesized and purified in a manner analogous to the synthesis of **1**, with 3-phenylpropylamine (0.388 mmol) as the amine component. Yield: 7 mg (4% overall, α:β = 29%:71%). ESI-MS m/z 460.9. For ^{1}H-NMR, all peaks corresponding to the core structure were observed and were consistent with those reported for compound **1** with the following additional peaks observed for the side chain: δ 7.35–7.2 (m, 5H, aromatic), 3.53–3.46 (quartet, 2H, aromatic), 2.78 (t, 2H, CH_2), and 2.02 (quintet, 2H, CH_2).

(3-nitro-5-(3-morpholin-4-yl-propylaminocarbonyl)phenyl)-galactopyranoside (**12**): compound **12** was synthesized and purified in a manner analogous to the synthesis of **1**, with N-(3-aminopropyl)morpholine (0.388 mmol) as the amine component. Yield: 17 mg (9% overall, α:β = 44%:56%). ESI-MS m/z 506.4 (chloride adduct), 583.9 (TFA adduct). For ^{1}H-NMR, all peaks corresponding to the core structure were observed and consistent with those reported for compound **1** with the following additional peaks observed for the side chain: δ 3.60 (t, 6H), 3.41–3.30 (m, 6H,), and 2.15 (quintet, 2H, CH_2).

(3-nitro-5-(3-(5-oxo-pyrrolidin-2-yl)-propylaminocarbonyl)phenyl)-galactopyranoside (**13**): compound **13** was synthesized and purified in a manner analogous to the synthesis of **1**, with 1-(3-aminopropyl)-2-pyrrolidinone (0.388 mmol) as the amine component. Yield: 17 mg (9% overall, α:β = 38%:62%). ESI-MS m/z 468.1. For ^{1}H-NMR, all peaks corresponding to the core structure were observed and were consistent with those reported for compound **1** with the following additional peaks observed for the side chain: δ 3.57 (t, 2H), 3.46 (t, 4H), 2.48 (t, 2H, CH_2), 2.14 (quintet, 2H, ring CH_2), and 1.94 (quintet, 2H, CH_2).

(3-nitro-5-(4-phenyl-butylaminocarbonyl)phenyl)-galactopyranoside (**14**): compound **14** was synthesized and purified in a manner analogous to the synthesis of **1**, with 4-phenylbutylamine (0.388 mmol) as the amine component. Yield: 3 mg (2% overall, α:β = 27%:73%). ESI-MS m/z 475.1. For ^{1}H-NMR, all peaks corresponding to the core structure were observed and consistent with those reported for compound **1** with the following additional peaks observed for the side chain: δ 7.33–7.18 (m, 5H, aromatic), 3.48 (t, 2H), 2.74 (t, 2H, CH_2), and 1.81–1.70 (m, 4H, CH_2).

(3-nitro-5-(4-pyren-1-yl-butylaminocarbonyl)phenyl)-galactopyranoside (**15**): compound **15** was synthesized and purified in a manner analogous to the synthesis of **1**, with 1-pyrenebutylamine (Toronto Research Chemicals, 0.388 mmol) as the amine component. Yield: 7 mg (4% overall, α:β = 33%:67%). ESI-MS m/z 599.0. For ^{1}H-NMR, all peaks corresponding to the core structure were observed and were consistent with those reported for compound **1** with the following additional peaks observed for the side chain: δ 8.4–7.92 (m, 9H, pyrene, obscuring aromatic protons of core structure), 3.56–3.38 (m, 4H), 2.02 (quintet, 2H, CH_2), 1.87 (quintet, 2H, CH_2).

Library Screening

The LTB_5 ELISA screening assay, including protein expression, purification, and characterization, was performed according to the established protocols of Minke [7]. The library compounds were dissolved in phosphate-buffered saline (pH 7.4) containing 10% DMSO. Compounds were screened as the anomeric mixture obtained after HPLC purification at 100 μM total (α + β) concentration. The working concentration of LTB_5 was 0.2 μg/ml for all samples, which were dispensed in quadruplicate and validated against a concentration gradient containing 0, 0.1, 0.2, and 0.3 μg/ml LTB_5.

Pulsed Ultrafiltration Experiments

Anomerically pure (α anomer only) samples of compounds **4** and **12** were obtained by the β-galactosidase digest/repurification protocol previously described [8]. Binding constants for these two compounds were determined via pulsed ultrafiltration (PUF) as described by Chen and Venton [10]. The working concentration of the ligands was determined spectroscopically at 218 nm by using an extinction coefficient of 16,180 $M^{-1}\cdot cm^{-1}$ obtained from dry weight analysis of **12**. The initial concentration of **4** and **12** (in 50 mM phosphate buffer) in the ultrafiltration cell was set to vary between 45 and 95 μM at the start of a given experiment. The LTB_5 concentration was either 1.6 μM, when the lower ligand concentration was used, or 3.2 μM, when the higher ligand concentration was used. For the MNPG control, a ligand concentration of 283 μM was used in conjunction with an LTB_5 concentration of 7.6 μM. The higher concentrations used for the MNPG experiments was required because of its lower affinity toward the toxin pentamer. The pulsed ultrafiltration cell was constructed from an in-line preparative HPLC solvent filter (Upchurch Scientific, Oak Harbor, WA; catalog number A-330), where the filter frit is replaced by a semi-permeable cellulose membrane (YM10, MWCO 10,000, 25 mm diameter; Amicon, Beverly, MA). The internal volume of the assembled cell was approximately 450 μl. Stirring was achieved by means of a small magnetic stir bar. Phosphate buffer (50 mM, pH 7.4) was used as the solvent at a flow rate of either 0.08 or 0.05 ml/min during the experiment. Elution of compounds from the cell was monitored at 230 nm.

Isothermal Titration Calorimetry

Isothermal titration calorimetry was performed with a Calorimetry Sciences Corporation (CSC model 4200) calorimeter with an internal cell volume of 1.305 ml. Experiments were designed according to guidelines from the CSC manual as well as from the work of Wiseman [19]. Anomerically pure samples of compounds **4** and **12** were obtained in the same manner as for the pulsed ultrafiltration experiments. The concentrations of ligand solutions were also determined in the same manner as described for the PUF experiments and varied from 75 to 125 μM in phosphate-buffered saline containing 50 mM sodium phosphate and 150 mM NaCl at pH 7.4. The initial concentration of porcine LTB_5 in the calorimeter cell varied from 15 to 20 μM in the same buffer. Experiments were conducted in overflow mode, and at least two separate ITC experiments were performed for each compound at 25°C. Curve fitting and determination of binding constants were performed with the BindWorks software included with the instrument.

Crystallization and Structure Determination

LTB_5 and CTB_5 were expressed and purified as described elsewhere [7]. Crystals of CTB_5 complexed with **4** grew from sitting drops consisting of 1 μl protein at 6.0 mg/ml in 50 mM Tris HCl at pH 7.4, 200 mm NaCl, 3 mm NaN_3, and 1 mm EDTA; 2 μl well buffer containing 50 mM NaCl, 100 mM Tris HCl at pH 7.5, and 30% PEG 3000. Crystals were isomorphous to the previously determined complex of CTB_5 with the GM1 pentasaccharide [20].

Crystals of LTB_5 complexed with **12** grew from sitting drops consisting of 2 μl protein at 2.0 mg/ml in 50 mM Tris HCl at pH 7.4, 200 mm NaCl, 3 mm NaN_3, and 1 mm EDTA; 2 μl well buffer containing 50 mM NaCl, 100 mM Tris HCl at pH 6.5, and 30% PEG 3000. Crystals were not isomorphous to any previously determined structure of either toxin pentamer.

X-ray intensities from a single flash-frozen crystal of each complex were measured with a wavelength of 1.0332 Å at the APS Structural Biology Center beamline 19ID. The data were integrated and scaled with the programs *HKL2000* and *TRUNCATE* [21, 22]. Initial molecular replacement solutions for three independent pentamers in the **12**:LTB_5 complex were found with the program *AMoRe* [23]; the starting structure was a previously refined structure for LTB_5 refined at 1.4 Å resolution (our unpublished data). Isotropic refinement of both complexes was carried out in *REFMAC* [24]. Model-fitting and placement and real-space refinement of ligands and water molecules were carried out with *XFIT* [25]. Initial anisotropic refinement of the **4**:CTB_5 complex, with atomic U^{ij} parameters for the protein atoms only, was carried out in *REFMAC* version 4.0. *REFMAC* refinement was not well behaved after the addition of atomic U^{ij} parameters for solvent molecules, so the model was shifted to *SHELXL* [26] for further refinement. The final rounds of refinement included anisotropic thermal parameters for all protein and water molecules. Water molecules were restrained toward isotropy (ISOR = 0.10). Ligand atoms were kept isotropic. Discrete disorder was modeled for six protein residues and for three of the five bound ligand molecules. The choice of restraint weights for U^{ij} parameters was guided by analysis of the overall distribution of anisotropy with *PARVATI* [27]. The statistical properties of the final crystallographic models are summarized in Table 1.

Acknowledgments

This work was supported in part by the National Institutes of Health (grant AI44954 to E.F.; grant AI34501 to WGJH; and grant GM54618 to C.V.) and by the Murdock Charitable Trust. We would like to thank Wendy Sanderson and Stewart Turley for assistance with calorimetry experiments. We thank the staff at SBC beamline 19ID, in particular Frank J. Rotella and Krzysztof Lazarski, for assistance in the data collection. Use of the Argonne National Laboratory Structural Biology Center beamlines at the Advanced Photon Source was supported by the U.S. Department of Energy, Office of Biological and Environmental Research, under contract number W-31-109-ENG-38.

Received: August 21, 2001
Accepted: November 6, 2001

References

1. Fan, E., Merritt, E.A., Verlinde, C.L.M.J., and Hol, W.G.J. (2000). AB_5 toxins: structures and inhibitor design. Curr. Opin. Struct. Biol. *10*, 680–686.
2. Spangler, B.D. (1992). Structure and function of cholera toxin and the related *Escherichia coli* heat-labile enterotoxin. Microbiol. Rev. *56*, 622–647.
3. Bernardi, A., Checchia, A., Brocca, P., Sonnino, S., and Zuccotto, F. (1999). Sugar mimics: an artificial receptor for cholera toxin. J. Am. Chem. Soc. *121*, 2032–2036.
4. Bhattacharya, S.K., and Danieshefsky, S.J. (2000). A total synthesis of the methyl glycoside of ganglioside GM_1. J. Org. Chem. *65*, 144–151.
5. Merritt, E.A., Sarfaty, S., Feil, I.K., and Hol, W.G.J. (1997). Structural foundation for the design of receptor antagonists targeting *Escherichia coli* heat-labile enterotoxin. Structure *5*, 1485–1499.
6. Minke, W.E., Hong, F., Verlinde, C.L.M.J., Hol, W.G.J., and Fan, E. (1999). Using a galactose library for exploration of a novel hydrophobic pocket in the receptor binding site of the *E. coli* heat-labile enterotoxin. J. Biol. Chem. *274*, 33469–33473.
7. Minke, W.E., Roach, C., Hol, W.G.J., and Verlinde, C.L.M.J. (1999). Structure-based exploration of the ganglioside GM1 binding sites of *E. coli* heat-labile enterotoxin and cholera toxin for the discovery of receptor antagonists. Biochemistry *38*, 5684–5692.
8. Fan, E., Merritt, E.A., Zhang, Z., Pickens, J., Roach, C., Ahn, M., and Hol, W.G.J. (2001). Exploration of the GM1 receptor binding site of heat-labile enterotoxin and cholera toxin by phenyl ring-containing galactose derivatives. Acta Crystallogr. *D57*, 201–212.
9. Rayle, H.L., and Fellmeth, L. (1999). Development of a process for triazine-promoted amidation of carboxylic acids. Organic Process Research & Development *3*, 172–176.
10. Chen, C.-J., Chen, S., Woodbury, C.P.J., and Venton, D.L. (1998). Pulsed ultrafiltration characterization of binding. Anal. Biochem. *261*, 164–182.
11. Chen, S. Further development of pulsed ultrafiltration analysis of ligand-macromolecule interactions. Ph.D. thesis, University of Illinois at Chicago.
12. Woodbury, C.P., and Venton, D.L. (1998). Pulsed ultrafiltration: a new method for screening and measuring ligand binding. Am. Lab. *30*, 16–19.
13. Zhao, Y.-Z., van Breemen, R.B., Nikolic, D., Huang, C.-R., Woodbury, C.P., Schilling, A., and Venton, D.L. (1997). Screening solution-phase combinatorial libraries using pulsed ultrfiltration/electrospray mass spectrometry. J. Med. Chem. *40*, 4006–4012.
14. Nikolic, D., Habibi-Goudarzi, S., Corley, D.G., Gafner, S., Pezzuto, J.M., and van Breemen, R.B. (2000). Evaluation of cyclooxygenase-2 inhibitors using pulsed ultrafiltration mass spectrometry. Anal. Chem. *72*, 3853–3859.
15. Thompson, J.P., and Schengrund, C.L. (1997). Oligosaccharide-derivatized dendrimers: defined multivalent inhibitors of the adherence of the cholera toxin B subunit and the heat labile enterotoxin of *E. coli* to GM1. Glycoconj. J. *14*, 837–845.
16. Fan, E., Zhang, Z., Minke, W.E., Hou, Z., Verlinde, C.L.M.J., and Hol, W.G.J. (2000). High affinity pentavalent ligands of *Escherichia coli* heat-labile enterotoxin by modular structure-based design. J. Am. Chem. Soc. *122*, 2663–2664.
17. Kitov, P.I., Sadowska, J.M., Mulvey, G., Armstrong, G.D., Ling, H., Pannu, N.S., Read, R.J., and Bundle, D.R. (2000). Shiga-like toxins are neutralized by tailored multivalent carbohydrate ligands. Nature *403*, 669–672.
18. Minke, W.E., Pickens, J., Merritt, E.A., Fan, E., Verlinde, C.L.M.J., and Hol, W.G.J. (2000). Structure of *m*-carboxyphenyl-α-D-galactose complexed to heat-labile enterotoxin at 1.3 Å resolution: surprising variations in ligand binding modes. Acta Crystallogr. *D56*, 795–804.
19. Wiseman, T., Williston, S., Brandts, J.F., and Lin, L.-N. (1989). Rapid measurement of binding constants and heats of binding using a new titration calorimeter. Anal. Biochem. *179*, 131–137.
20. Merritt, E.A., Sarfaty, S., van den Akker, F., L'hoir, C., Martial, J.A., and Hol, W.G.J. (1994). Crystal structure of cholera toxin B-pentamer bound to receptor GM1 pentasaccharide. Protein Sci. *3*, 166–175.
21. Otwinowski, Z., and Minor, W. (1997). Processing of X-ray diffraction data collected in oscillation mode. Methods Enzymol. *276*, 307–326.
22. CCP4 (Collaborative Computational Project 4). (1994). The CCP4 suite: programs for protein crystallography. Acta Cryst. D *50*, 760–763.
23. Navaza, J. (1994). AMoRe: an automated package for molecular replacement. Acta Crystallogr. A *50*, 157–163.
24. Murshudov, G.N., Vagin, A.A., Lebedev, A., Wilson, K.S., and Dodson, E.J. (1999). Efficient anisotropic refinement of macromolecular structures using FFT. Acta Crystallogr. D *55*, 247–255.
25. McRee, D. (1993). Practical Protein Crystallography. (San Diego, CA: Academic Press).

26. Sheldrick, G.M., and Schneider, T.R. (1997). SHELXL: high-resolution refinement. Methods Enzymol. *227*, 319–343.
27. Merritt, E.A. (1999). Expanding the model: anisotropic displacement parameters in protein structure refinement. Acta Crystallogr. *D55*, 1109–1117.
28. Merritt, E.A., and Bacon, D.J. (1997). Raster3D: photorealistic molecular graphics. Methods Enzymol. *277*, 505–524.

Accession Numbers

Crystal structure coordinates for compounds **4** and **12** in complex with the toxin B pentamers have been deposited in the Protein Data Bank (PDB entry code 1jr0 and 1jqy, respectively).